https://doi.org/10.5194/egusphere-2026-3788
Preprint. Discussion started: 13 August 2026

Contrasting Arctic Cirrus Clouds: Properties and Processes from Observations and Simulations

Georgios Dekoutsidis[1], Silke Groß[1], Florian Ewald[1], Martina Krämer[3,4], Christian Rolf[2], Andreas Schäfler[1], Martin Wirth[1]

[1]Institut für Physik der Atmosphäre, Deutsches Zentrum für Luft- und Raumfahrt (DLR), Oberpfaffenhofen, 82234 Wessling, Germany
[2] Institute of Climate and Energy Systems (ICE-4), Research Center Jülich, 52425 Jülich, Germany
[3] Institute for Physics of the Atmosphere (IPA), Johannes-Gutenberg-Universität Mainz, 55128 Mainz, Germany
[4] formerly at [2]

Correspondence to: Georgios Dekoutsidis (georgios.dekoutsidis@dlr.de)

Abstract.

Cirrus clouds in the Arctic play a central role in the regional radiation budget, yet their formation pathways and properties remain poorly constrained, especially during Warm Air Intrusions (WAI). In this study, we analyse and contrast cirrus observed during WAI events (WAI cirrus) with those formed under undisturbed Arctic Conditions (AC cirrus) using remote sensing measurements from the HALO–(AC)³ campaign, combined with backward trajectory modelling with CLaMS-Ice and LAGRANTO. This allows us to connect the optical, macro- and microphysical properties measured via lidar and radar to the cloud origin and dynamics during their evolution. We find that WAI cirrus encountered stronger vertical transport along their trajectories compared to AC cirrus. At the time of detection, WAI cirrus were geometrically and optically thicker, exhibited higher depolarization ratios and ice supersaturation, and contained more numerous but smaller ice crystals, consistent with homogeneous ice nucleation at colder temperatures. AC cirrus, in contrast, showed larger ice crystals and a comparably greater contribution from heterogeneous ice nucleation. As WAI events are projected to become more frequent and long-lasting, a resulting increase in the formation of WAI cirrus may enhance their influence on the Arctic radiation budget leading to cooling. Our results provide observational constraints on cirrus variability in the Arctic and emphasize the need for their improved representation in weather and climate models.

1 Introduction

The Earth's climate is undergoing changes. Global warming, the continuous rise in Earth's average global temperature, has been thoroughly studied and is backed by scientific evidence. . The Arctic, due to its remoteness and low population density, is one of the less studied regions, but still remains one of great interest, complexity, impact and unanswered questions. In recent decades, measurements have shown a much faster rate of warming in the Arctic compared to the global average. This phenomenon is named Arctic Amplification (Serreze and Francis, 2006; Woods and Caballero, 2016; Richter-Menge et al., 2018; Wendisch et al., 2023). The accelerated warming of the Arctic, leads to a weakening of the polar jet stream. This in turn

https://doi.org/10.5194/egusphere-2026-3788
Preprint. Discussion started: 13 August 2026

results in it having a wavier structure, and thus more frequently allowing airmasses from the mid-latitudes to intrude into the Arctic (Pithan et al., 2018; Stendel et al., 2021; Wendisch et al., 2025). These events, referred to as Warm Air Intrusions (WAI), are characterized by the meridional transport of warm, moisture- and aerosol-rich air masses from the mid-latitudes into the otherwise cold, dry, and relatively pristine Arctic. (Woods and Caballero, 2016). These events fuel the Arctic with energy, water vapor - a strong greenhouse gas - and aerosols, and cause significant changes, such as an increased cloud formation, especially in winter (Johansson et al., 2017).

Clouds affect the radiative balance of the atmosphere and can have a warming or cooling effect (Shupe and Intrieri, 2004). Cirrus clouds in particular, are found at high altitudes, are made up of ice crystals and are generally optically thin. They let a large portion of the incoming solar radiation through, while efficiently trapping the outgoing thermal radiation (Lynch, 2002). Thus, they can strongly contribute to the cloud greenhouse effect and enhance the rise of surface temperatures (Intrieri et al., 2002). Their exact effect and its amplitude are dependent on factors such as season, time of day, solar zenith angle, surface albedo, all with great variations in the Arctic and potentially causing a significant effect. The cirrus macro- and microphysical properties, such as number, size and shape of ice crystals, also play an important role in their effects (Mitchell et al., 2018, 2020; Marsing et al., 2023). These properties are in-turn affected by the type of airmass in which they form and evolve, the ambient meteorological conditions as well as the abundance and type of available aerosols (Comstock et al., 2008; Cziczo et al., 2013; Luebke et al., 2013; Urbanek et al., 2017, 2018; Dekoutsidis et al., 2023; De La Torre Castro et al., 2023).

Ice crystals can form via one of two nucleation pathways, homogeneous (HOM) or heterogeneous (HET). The ice nucleation mechanism is strongly influenced by the ambient conditions and produces ice crystals with different properties. HOM nucleation requires high supersaturations and very cold temperatures, while HET nucleation can be initiated at warmer temperatures, provided that the right amount and type of aerosols, Ice Nucleating Particles (INPs) are present (Koop et al., 2000; Kärcher and Lohmann, 2002, 2003; Hoose and Möhler, 2012). Regarding their formation process, Krämer et al. (2016) and Luebke et al. (2016) propose that ice clouds can either form directly into the ice phase (in-situ-origin) or evolve from a liquid predecessor cloud (liquid-origin), based once again largely on the ambient conditions. The distinction between the two cloud formation pathways is important as they lead to clouds with different microphysical properties and radiative effects. Liquid origin cirrus generally have a larger ice water content (IWC) and larger ice crystal number and sizes, and thus have on average a cooling effect (Krämer et al., 2016, 2020; Luebke et al., 2016).

Warm Air intrusions, can significantly alter the ambient conditions in which cirrus clouds form in the Arctic and thus lead to differences in their formation, properties and effects (Pithan et al., 2018; Dekoutsidis et al., 2023, 2024). WAI events have been increasing in frequency and duration in connection with Arctic Amplification, and are projected to continue their positive trend (Graham et al., 2017). This can lead to more cirrus clouds being formed under these previously less common conditions, with less well-known properties and effects, different to the common Arctic cirrus. Dekoutsidis et al. (2024), characterize the clouds that form during an intrusion event as WAI cirrus, and the ones that form in undisturbed Arctic Conditions as AC cirrus. Cirrus clouds are already commonly underrepresented and oversimplified in many weather and climate models and even more so WAI cirrus, despite their increasing relevance in the process and feedbacks taking place in the Arctic (DeMott et al., 2010;

https://doi.org/10.5194/egusphere-2026-3788
Preprint. Discussion started: 13 August 2026

Gasparini et al., 2018). The first step towards a better representation, parametrization and understanding of those clouds, is to perform measurements, which, up to now, are rare in the Arctic, compared to other regions (De La Torre Castro et al., 2023). The HALO-(AC)^3 campaign, during which remote sensing measurements, with the German research aircraft HALO were performed over the Arctic, was a successful effort in this direction (Krautstrunk and Giez, 2012; Wendisch et al., 2024; Ehrlich et al., 2025).

In this work, our aim is to provide a detailed study and comparison of the optical, macro- and microphysical properties of AC and WAI cirrus in the Arctic. We use radar and lidar measurements of cirrus clouds performed during the HALO-(AC)^3 campaign and two models that provide Lagrangian backwards trajectories. This way we can perform an all-around study from cloud formation to detection.

2 Data and method

2.1 HALO-(AC)^3

The HALO-(AC)^3 (Arctic Air Mass Transformations during Warm Air Intrusions and Marine Cold Air Outbreaks) flight campaign was conducted, in spring of 2022 in the Arctic (Ehrlich et al., 2025). A primary objective of the campaign was to investigate air mass transformation processes and WAI events (Wendisch et al., 2024). For this purpose, measurement flights were performed with the German research aircraft HALO and the polar aircrafts P5 and P6. HALO is a Gulfstream G500 business jet, specifically modified to perform atmospheric measurements (Krautstrunk and Giez, 2012; Stevens et al., 2019).

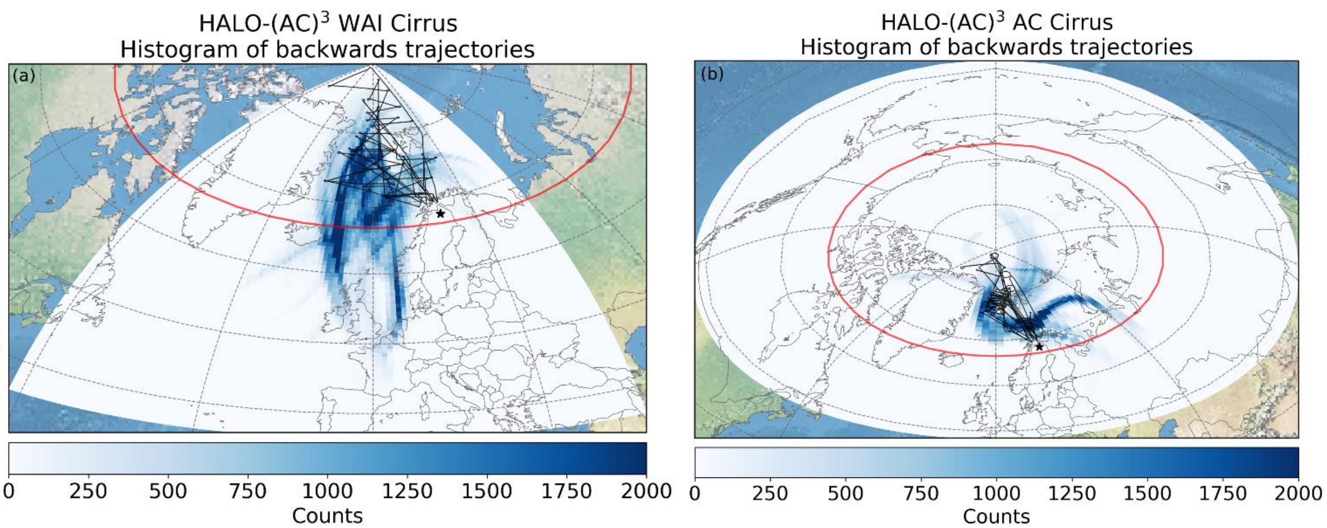

Figure 1: Flight tracks and histogram of the 24h backwards trajectories as calculated by CLaMS-Ice for Warm Air Intrusion (WAI) cirrus (Left) and Arctic Condition (AC) cirrus (Right). The red line represents the Arctic circle. The star represents the airport of Kiruna, Sweden.

Its long range and high flight ceiling make it an exceptional platform for the study of high-altitude cirrus clouds at remote locations, such as the Arctic (Groß et al., 2014; Urbanek et al., 2018; Dekoutsidis et al., 2023). For this campaign HALO was

https://doi.org/10.5194/egusphere-2026-3788
Preprint. Discussion started: 13 August 2026

equipped with a suite of active and passive remote sensing instruments, including the combined water vapor differential absorption and high spectral resolution lidar system WALES and the HAMP microwave package including a cloud radar (MIRA-35) and radiometers (Wirth et al., 2009; Mech et al., 2014; Ewald et al., 2019).

2.2 Measurement dataset

This study is based on a dataset of ice cloud parameters created from measurements performed by the WALES lidar system during the HALO-(AC)^3 campaign. These parameters include i) the backscatter ratio, which was used to identify the clouds and determine their top and base, ii) the water vapor mixing ratio, which combined with model temperatures provides the Relative Humidity over ice (RHi), iii) the optical transmission, from which the cloud optical depth (OD) is calculated and iv) the Particle Linear Depolarization Ratio (PLDR) used directly to characterize the ice crystals.

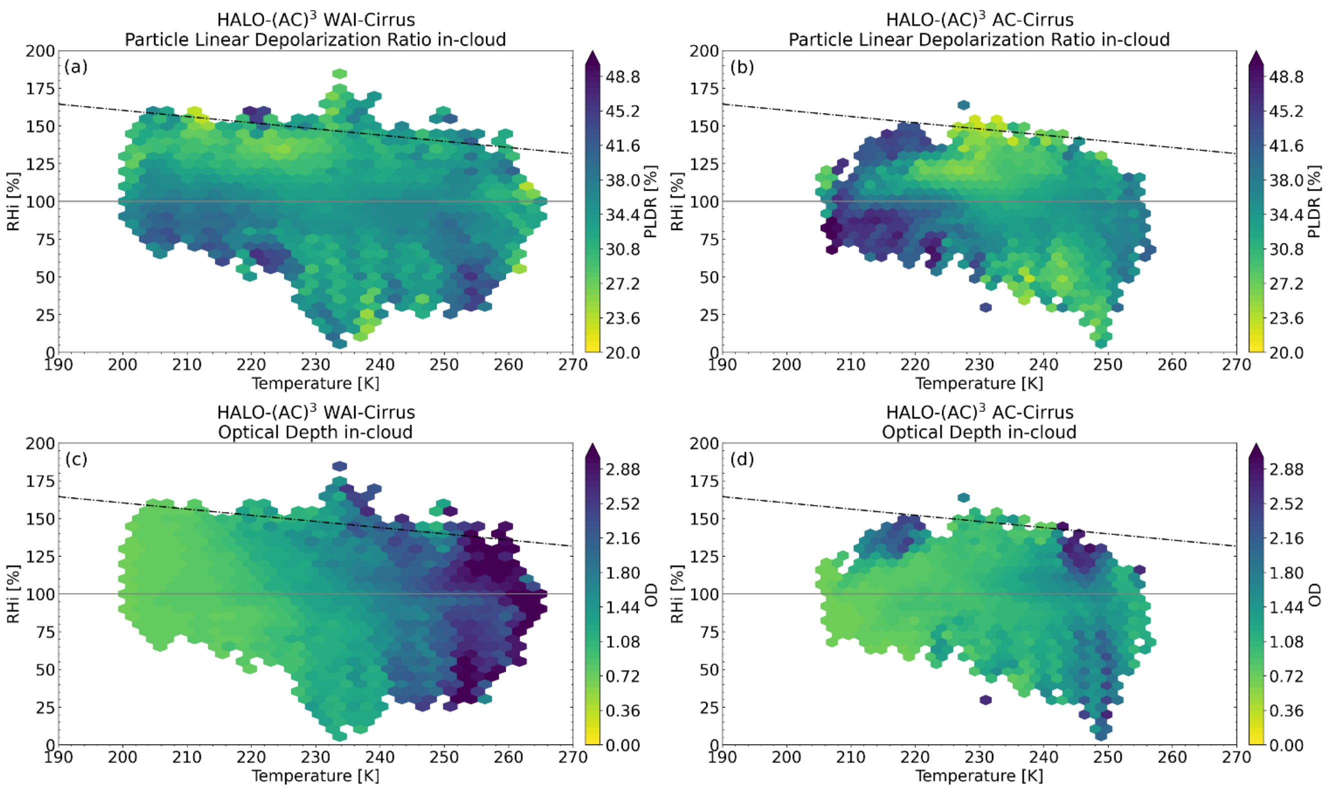

Figure 2: Particle Linear Depolarization Ratio (PLDR) and Optical Depth (OD) measured by the WALES lidar system, during the HALO-(AC)^3 campaign on axis of Temperature from ECMWF model calculations, against Relative Humidity over ice (RHi) calculated from the WALES water vapor measurements and model temperatures. Left: Warm Air Intrusion (WAI) cirrus. Right: Arctic Condition (AC) cirrus. The solid grey line depicts the threshold for ice saturation (RHi = 100 %). The black dash-dotted line represents the homogeneous nucleation (HOM) threshold based on Koop et al. (2000).

The measurement dataset was split into two groups, one containing Warm Air Intrusion (WAI) cirrus and the other containing Arctic Condition (AC) cirrus. A total of 9 research flights amassing around 61 hours of measurements were classified as Arctic

Conditions (AC) providing 684967 in-cloud data points. 6 research flights including almost 44 hours of measurements and 895345 in-cloud data points were classified as Warm Air Intrusion (WAI).

In Fig. 2 we present the measured particle linear depolarization ratio and cloud optical depth from WALES in the RHi-T space for the two cloud groups, WAI and AC cirrus. We can already point out the wider temperature range in which WAI cirrus have been detected. WAI cirrus are also detected more frequently at the HOM threshold, especially at colder temperatures. Both cloud types have high depolarization ratios indicative of ice crystals with complex shapes or aggregates, at the colder end of the temperature range and in subsaturation. AC cirrus have a region of high depolarization also at cold temperatures and high supersaturations near the HOM threshold. The optical depth for WAI cirrus follows the expected pattern and increases with temperature. AC cirrus have a region of elevated OD coinciding with the area of high depolarization ratio, indicative of an active ice-forming region.

2.3 Methodology

Our first step was to classify the cirrus clouds measured during HALO-(AC)^3 by WALES and HAMP as either AC or WAI cirrus depending on if they formed in undisturbed Arctic Conditions or during a WAI event. For this, we qualitatively evaluated parameters such as ambient temperature and available water vapor and also took into consideration the backwards trajectories. In Fig. 1 we present maps with the 24-hour backwards trajectories calculated by CLaMS-Ice, using the cirrus clouds detected by WALES as the starting point. It is evident, that cirrus clouds classified as WAI cirrus tend to have airmasses transferred from the mid-latitudes, while clouds classified as AC cirrus formed in Arctic airmasses. Having created the two cirrus cloud groups, our aim was to compare their characteristics. The geometrical, optical and macrophysical properties were provided by the WALES lidar and MIRA-35 cloud radar measurements. For the microphysical properties the VarCloud retrieval was employed, which uses measurements from the lidar and radar instruments.

Finally, in order to retrieve information on the conditions during formation and evolution of AC and WAI cirrus we used two models. The Lagrangian analysis tool LAGRANTO was used to calculate the 100-hour backwards trajectories of the clouds detected from the synergy between the WALES lidar and MIRA-35 cloud radar. The CLaMS-Ice model, which combines the trajectory tool of the Chemical Lagrangian Model of the Stratosphere (CLaMS) with two-moment ice microphysics, was used to calculate the 24-hour backwards trajectories for the cirrus clouds in the two groups and the microphysical properties along those trajectories.

2.3.1 VarCloud

To derive ice cloud microphysics from the combination of WALES and MIRA-35 measurements we used the optimal estimation framework VarCloud (Delanoë and Hogan, 2008). This retrieval framework was originally developed for the ice cloud product DARDAR (Delanoë and Hogan, 2010) which combines data from the CALIOP lidar on CALIPSO (Winker et al., 2010) with the cloud profiling radar CPR on CloudSat (Stephens et al., 2008). The assumptions about the ice crystal model

https://doi.org/10.5194/egusphere-2026-3788
Preprint. Discussion started: 13 August 2026

were described in Cazenave et al. (2019) and the retrieval was transferred to HALO observations by Ewald et al. (2021) which validated the retrieved ice microphysics via in situ measurements and radiative closure with additional passive measurements.

2.3.2 CLaMS-Ice

CLaMS-Ice is a Lagrangian cirrus cloud microphysics model (Luebke et al., 2016; Baumgartner et al., 2022), designed to simulate the evolution of ice microphysical properties along air parcel trajectories. Air parcel backwards trajectories are calculated using the Chemical Lagrangian Model of the Stratosphere (CLaMS; McKenna et al., (2002)) .The starting point can be an arbitrary location in the atmosphere. In this study it is provided by WALES measurements. The trajectory calculations are driven by ERA5 wind fields from the European Centre for Medium-Range Weather Forecasts (ECMWF), while diabatic heating rates are used to represent vertical motion. The default time frame of the trajectories for cirrus clouds is 24 hours. To account for unresolved small-scale temperature variability that is not captured by the coarse ERA5 resolution, additional temperature perturbations following Podglajen et al. (2016) are superimposed.

The CLaMS-Ice model then simulates the evolution along the trajectories forward in time. The initial water is taken from ERA5, which is then distributed between cloud particles and the gas phase using the two-moment box-model developed by Spichtinger and Gierens, (2009). This framework represents the formation and evolution of cirrus clouds by including homogeneous ice nucleation (following Koop et al. (2000)) as well as heterogeneous freezing, growth of ice crystals by deposition, and their evaporation, aggregation, and sedimentation (sedimentation parametrization after Spichtinger and Gierens, (2009); the sedimentation parameter is set to 0.97). Homogeneous freezing is controlled by the concentration of supercooled solution droplets, which is configurable and set to 300 cm^{-3} by default Heterogeneous freezing is initiated once a critical ice supersaturation of 120% is exceeded. For each freezing pathway, the model predicts the: ice number concentration (ICN) and ice water content (IWC).

Only trajectories terminating at temperatures below 238 K are treated with the standard two-moment scheme. If a trajectory originates at temperatures above 238 K before entering the colder cirrus regime, the simulation is initialized at 238 K using pre-existing ice water content derived from mixed-phase clouds, provided that such clouds are identified in the ERA5 data between 240 K and 238 K. The IWC is converted to ice number concentration using a parameterization (Costa, 2017), then CLaMS-Ice proceeds as for newly formed cirrus clouds. While the trajectories are initiated at the locations where, WALES detected an ice cloud, since CLaMS-Ice uses its own fields, it might be the case that, some trajectories are found with no ice cloud detected.

Following Krämer et al. (2016) and Luebke et al. (2016), pre-existing ice found between 240 K and 230 K, accounting for fast updrafts or convection, is defined as, liquid-origin cirrus‘. Liquid-origin ice crystals are assumed to form heterogeneously and to release an INP once they evaporate. Ice clouds that form during the course of the trajectory at T < 238 K without initial liquid-origin cirrus are called ‘in situ-origin’ cirrus. If a back trajectory ends at T < 238 K and pre-existing ice is found, it is not possible to assign it to liquid-origin or in-situ-origin cirrus; this category is called 'unknown-origin'.

https://doi.org/10.5194/egusphere-2026-3788
Preprint. Discussion started: 13 August 2026

2.3.3 LAGRANTO

The Lagrangian Analysis Tool (LAGRANTO) is a model for the calculation of three-dimensional air parcel trajectories. It has been extensively documented and validated on many applications, including the study of ice clouds (Wernli and Davies, 1997; Sprenger and Wernli, 2015; Wernli et al., 2016). In this study, the calculations are driven by gridded wind fields from the ERA5 reanalysis dataset of ECMWF. The trajectories are initialized at every observation location of the VarCloud dataset following an approach described in Schäfler et al. (2023), that accounts for the variable time of the starting locations.

Tracing meteorological parameters (e.g. temperature, pressure, Ice Water Content (IWC), Liquid Water Content (LWC), vertical velocity) along the trajectories enables the identification cloud formation pathways and estimation of cloud age by determining when air parcels first satisfy specific microphysical thresholds and others. Here, we only use trajectories providing a pure ice cloud at the starting location, which is defined by the Ice Water Content (IWC) and Liquid Water Content (LWC) being IWC > 0.1 mg kg^{-1} and LWC < 0.01 mg kg^{-1}. On the backwards trajectories an ice cloud is considered to have formed at the earliest time when IWC > 0.1 mg kg^{-1}. If at this time and along the whole trajectory there is no liquid water i.e. LWC < 0.01 mg kg^{-1} this ice cloud is characterized as an in-situ origin cirrus. Otherwise it is classified as a liquid origin cirrus.

2.3.4 Model comparison

To study the history of the WAI and AC cirrus detected during the HALO-$(AC)^3$ campaign we use two models, CLaMS-Ice and LAGRANTO. While there are many similarities between them and between the way they are used in this study, it is important to note that the two have different strengths and weaknesses and a different scope in this study. Most importantly LAGRANTO is a purely kinematic tool. It does not explicitly simulate microphysical processes, but traces variables as represented in the ERA5 meteorological fields and thus is limited to the representation of clouds in the model simulations. However, airmass transport can be studied through the complete range of temperatures. CLaMS-Ice on the other hand has the advantage of providing a more representation of microphysics of cirrus clouds in the temperature range < 238 K. However, because of the limitation to cirrus cloud processes it does not include the warmer parts where the cloud base is frequently found, in case of underlying mixed-phase clouds. For the distinction between in situ-origin and liquid-origin cirrus, we analyse the temperature range > 235 K.

In both models, the trajectory accuracy depends on the spatial and temporal resolution of the underlying fields, which may not fully resolve small-scale processes that are critical for ice formation. A main difference between LAGRANTO and CLaMS-Ice in that aspect, is that CLaMS-Ice considers small-scale temperature fluctuations, which are not represented in ERA5 used by LAGRANTO. Since the microphysics is driven mostly by the magnitude of the small-scale temperature changes, this needs to be considered when comparing, for example the IWC from the two models.

https://doi.org/10.5194/egusphere-2026-3788
Preprint. Discussion started: 13 August 2026

3 Results

In this chapter we present the findings from the statistical analysis of the two cirrus cloud groups (AC and WAI cirrus) detected during the HALO-(AC)[3] campaign. We focus on three main areas of interest. First, the formation of the clouds and the conditions along their trajectories, second their optical, macro- and microphysical properties at the time of detection, t0, and third their classification based on their origin and ice nucleation process.

3.1 Cloud formation and conditions along the backwards trajectories

We start by looking into the conditions and dynamical processes taking place during the cloud formation and evolution until their detection. Both CLaMS-Ice and LAGRANTO are used for this part of the analysis. It should be kept in mind, that the LAGRANTO trajectories run backwards for 100 hours and retrieve cloud properties from the ERA5 reanalysis dataset, while the CLaMS-Ice trajectories run for 24 hours, and include a two-moment microphysics scheme for cirrus clouds occurring at T < 238 K; thus lower, warmer parts of the clouds are not being represented in the simulations. In Table 1, we present the comparison of the median values of all listed parameters for the AC cirrus and WAI cirrus groups. Fig. 2 and 3 contain a

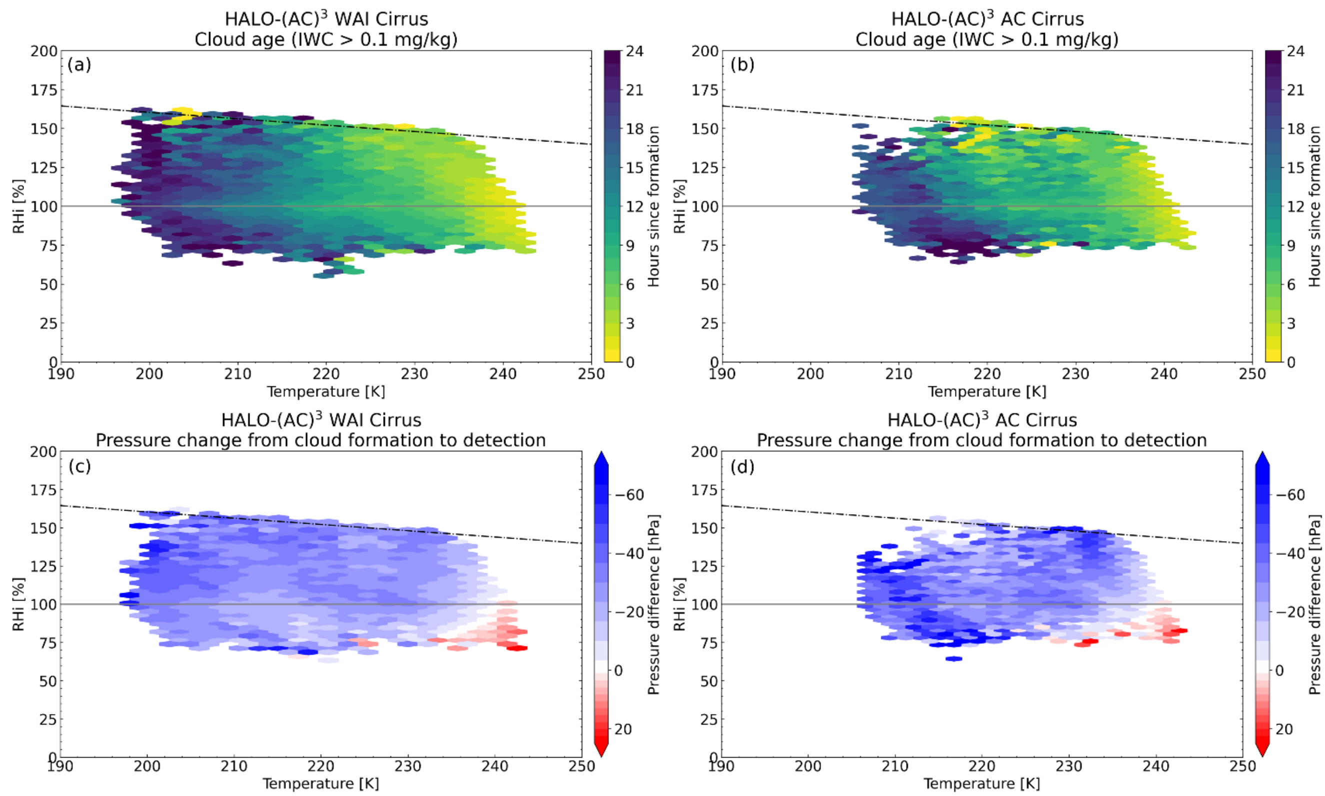

Figure 3: Comparison of Warm Air Intrusion (WAI Cirrus; Left) and Arctic Condition (AC Cirrus; Right) data from CLaMS-Ice simulations along the backwards trajectories in the RHi-T space. The solid grey line depicts the threshold for ice saturation (RHi = 100 %). The black dash-dotted line represents the homogeneous nucleation (HOM) threshold based on Koop et al. (2000).

https://doi.org/10.5194/egusphere-2026-3788
Preprint. Discussion started: 13 August 2026

Table 1: Cumulative results from all available datasets comparing Warm Air Intrusion (WAI) cirrus and Arctic Condition (AC) cirrus detected during the HALO-(AC)³ campaign. Data sources: ^{C}: CLaMS-Ice, ^{L}: LAGRANTO, ^{V}: VarCloud, ^{W}: WALES. All values are medians for the respective cloud group, WALES and geometrical depths are means.

		AC cirrus	WAI cirrus	Difference %
Formation, conditions and dynamics along the backwards trajectories	Cloud age [H]	7^{C}	7^{C}	0
	(First time backwards with IWC < 0.1 mg/kg)	18^{L}	17^{L}	-5.6
	Pressure difference from formation to detection [hPa]	-18.18^{C}	-19.89^{C}	-9.4
	Pressure change [hPa] since:			
	Formation	-42.8^{L}	-52.5^{L}	-22.7
	Last 3h	-4^{L}	-6.7^{L}	-67.5
	Last 6h	-7.8^{L}	-14.4^{L}	-84.6
	Mean vertical velocity **ω** [Pa/s] since:			
	Formation	-19.3^{L}	-28.2^{L}	-46.1
	Last 3h	-3.6^{L}	-6.2^{L}	-72.2
	Last 6h	-3.6^{L}	-6.5^{L}	-80.6
Microphysical, macrophysical and optical properties at time of detection (t0)	Geometrical depth [m]	2016^{W}	3065^{W}	52.1
		1864^{V}	2560^{V}	37.3
	Relative Humidity over Ice [%]	99.55^{W}	102.43^{W}	2.9
	Particle Linear Depolarization Ratio [%]	34.48^{W}	35.09^{W}	1.8
	Optical Depth	1.335^{W}	2.177^{W}	63.1
	Cloud Ice Mixing Ratio (**IWC**) [mg/kg]	6.57^{V}	8.76^{V}	33.3
	Cloud Ice Mixing Ratio (**IWC**) [mg/kg]	3.4^{L}	4.8^{L}	41.2
	Cloud Ice Mixing Ratio (**IWC**) [mg/kg]			
	Heterogeneous freezing class	$1.41\cdot10^{-5}$ ^{C}	$5.81\cdot10^{-4}$ ^{C}	4024.3
	Homogeneous freezing class	$1.06\cdot10^{-2}$ ^{C}	1.99^{C}	18717.4
	Total	$1.06\cdot10^{-2}$ ^{C}	1.99^{C}	18697.9
	Cloud Ice Effective Radius (**R_{eff}**) [µm]	49.3^{V}	44.2^{V}	-10.5
	Ice Crystal Number Concentration (**ICN**) [1/kg]			
	Heterogeneous freezing class	0.1^{C}	3.7^{C}	3600
	Homogeneous freezing class	50^{C}	$2.40\cdot10^{4}$ ^{C}	47900
	Total	50.1^{C}	$2.40\cdot10^{4}$ ^{C}	47811.6

https://doi.org/10.5194/egusphere-2026-3788
Preprint. Discussion started: 13 August 2026

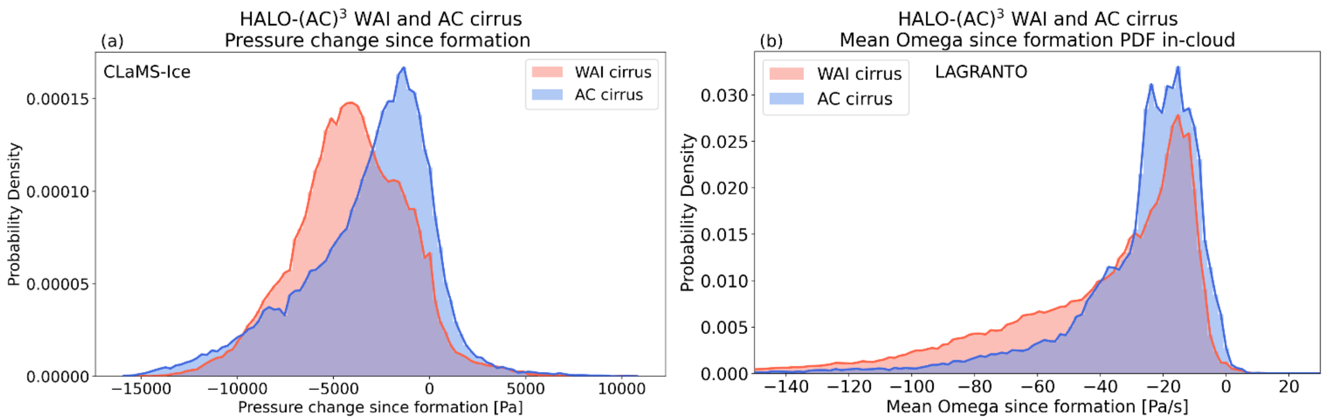

Figure 4: Comparison of probability densities of vertical motion along the backwards trajectories of Warm Air Intrusion (WAI Cirrus) and Arctic Condition (AC Cirrus) as calculated by CLaMS-Ice and LAGRANTO.

more detailed representation of similar parameters from WALES and CLaMS-Ice respectively in the RHi-T space, aiding to a more in-depth understanding.

The formation time is calculated with both models and is defined in both cases as the first instance along the trajectory with an ice water content (IWC) greater than 0.1 mg/kg. According to the CLaMS-Ice calculations, the two cloud types have on average the same age, whereas LAGRANTO finds WAI cirrus to be slightly younger, compared to AC cirrus. The difference in the lead times between the calculations of the two models should be kept in mind. Cloud age must be considered as most cloud properties, be it macro-, microphysical or optical are bound to change with time. Since the two cloud types are found to have rather similar ages on average we can be confident that age is not introducing any significant bias and the differences in the measured clouds, stem from the different conditions and processes during cloud formation and evolution.

A more in-depth view into the ages of AC and WAI cirrus is given in Fig. 3 (a) and (b). For both cloud types, there is a transition from older to younger parts while the temperatures decrease. Younger cloud-parts are found mostly above 215 K in a wide range of Relative Humidity over ice (RHi). They are followed at colder temperatures by the oldest parts of the clouds also throughout the range of RHi. Finally, in both cloud types at the colder and highly ice supersaturated regions there seem to be the youngest parts. This is a possible indication of HET and HOM nucleation in the warmer and colder regions respectively.

Regarding the vertical motion for the airmasses of the two cloud types, we use the change in ambient atmospheric pressure between cloud formation and detection, both from CLaMS-Ice and LAGRANTO, as well as the mean vertical velocities ω, provided by LAGRANTO. As shown in Table 1 and Fig. 4, both models agree, that WAI cirrus had a greater change in atmospheric pressure, i.e. a greater vertical movement. From LAGRANTO we find that WAI cirrus traveled a greater vertical distance and with a higher vertical velocity (Table 1 and Fig. 4).

In Fig. 3 (c) and (d), we present the change in atmospheric pressure simulated by CLaMS-Ice along the trajectories from cloud formation time to detection (t0) in the RHi-T space. For both cloud types the trajectories with the most pronounced vertical

https://doi.org/10.5194/egusphere-2026-3788
Preprint. Discussion started: 13 August 2026

motion are found at the colder end of the temperature range, indicating a transport to higher altitudes. In both WAI and AC cirrus there are also some trajectories with a downwards motion. These are found at the warmest end of the distribution and in slight subsaturation.

3.2 Cloud optical, macro- and microphysical properties at time of detection (t0)

In this section we compare the properties of AC and WAI cirrus at the time of detection, t0. First, we use measurements from the WALES lidar system and retrievals from VarCloud and calculate the average geometrical depth of the two cloud types. As shown in Table 1, both methods agree, that WAI cirrus are on average thicker than AC cirrus. Further analysis (not shown in Table 1) revealed, that the difference is mostly due to a higher altitude reached at cloud top, while the average cloud base

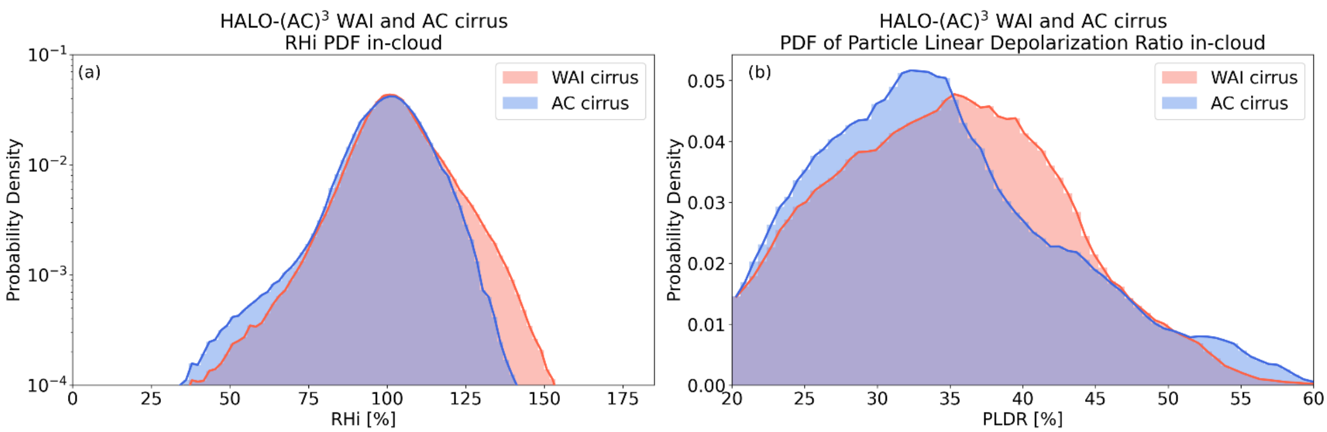

Figure 5: Comparison of WALES Relative Humidity over ice (RHi) and Particle Linear Depolarization Ratio (PLDR) between Warm Air Intrusion (WAI Cirrus) and Arctic Condition (AC Cirrus) measured during the HALO-(AC)³ campaign.

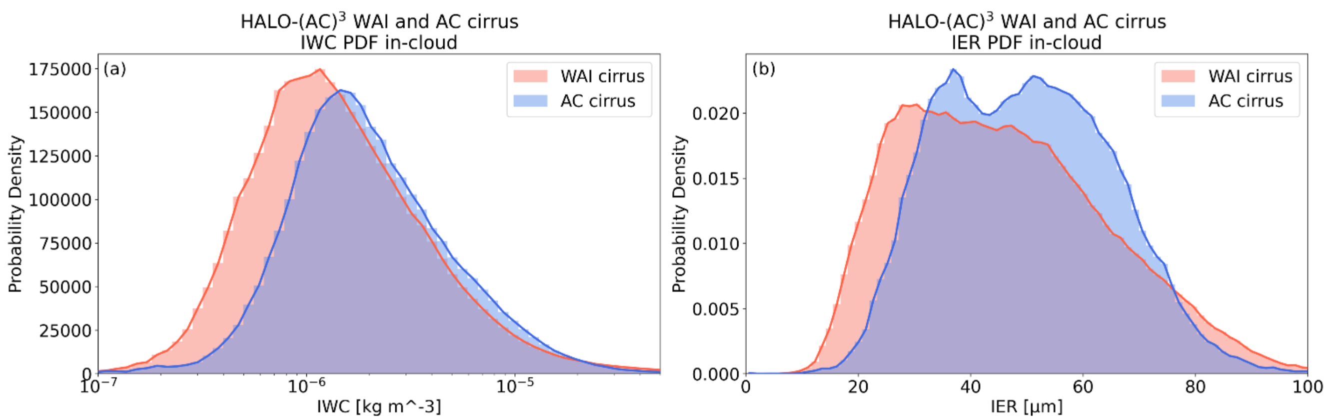

Figure 6: Comparison of probability densities of Ice Water Content (IWC) and Ice Effective Radius (R_{eff}) of Warm Air Intrusion (WAI Cirrus) and Arctic Condition (AC Cirrus) at t0 by VarCloud.

https://doi.org/10.5194/egusphere-2026-3788
Preprint. Discussion started: 13 August 2026

heights are closer between the two groups. An indication therefore can be seen in Figs 2,3 and 7, where both groups reach a similar temperature on the warmer end, while WAI cirrus reach lower temperatures compared to AC cirrus, indicative of a higher altitude.

We continue our analysis using measurements and products from WALES and compare the Relative Humidity over Ice (RHi), the Particle Linear Depolarization Ratio and Optical Depth (OD) in Figs 2 and 5 and Table 1. For both AC and WAI cirrus the RHi distribution peaks at around saturation, or 100 % RHi. That being said, WAI cirrus are more frequently measured at higher supersaturations, which would be required for homogeneous ice nucleation. As shown in Table 1 and Figure 5 (b), WAI cirrus also have on average a slightly higher PLDR, indicating more aspherical ice crystal shapes or aggregates. The final parameter we compare based on WALES measurements is the optical depth of the two cloud groups. As shown in Table 1 and Fig.2 (c) and (d), WAI cirrus have on average a greater optical depth. This comes as a result of the processes that took place during their formation, it is linked to the greater geometrical depth but can also have implications on their radiative properties and potential impact on the radiation budget in the Arctic. In Fig. 2 (c) and (d) we see that the OD steadily increase at higher temperatures

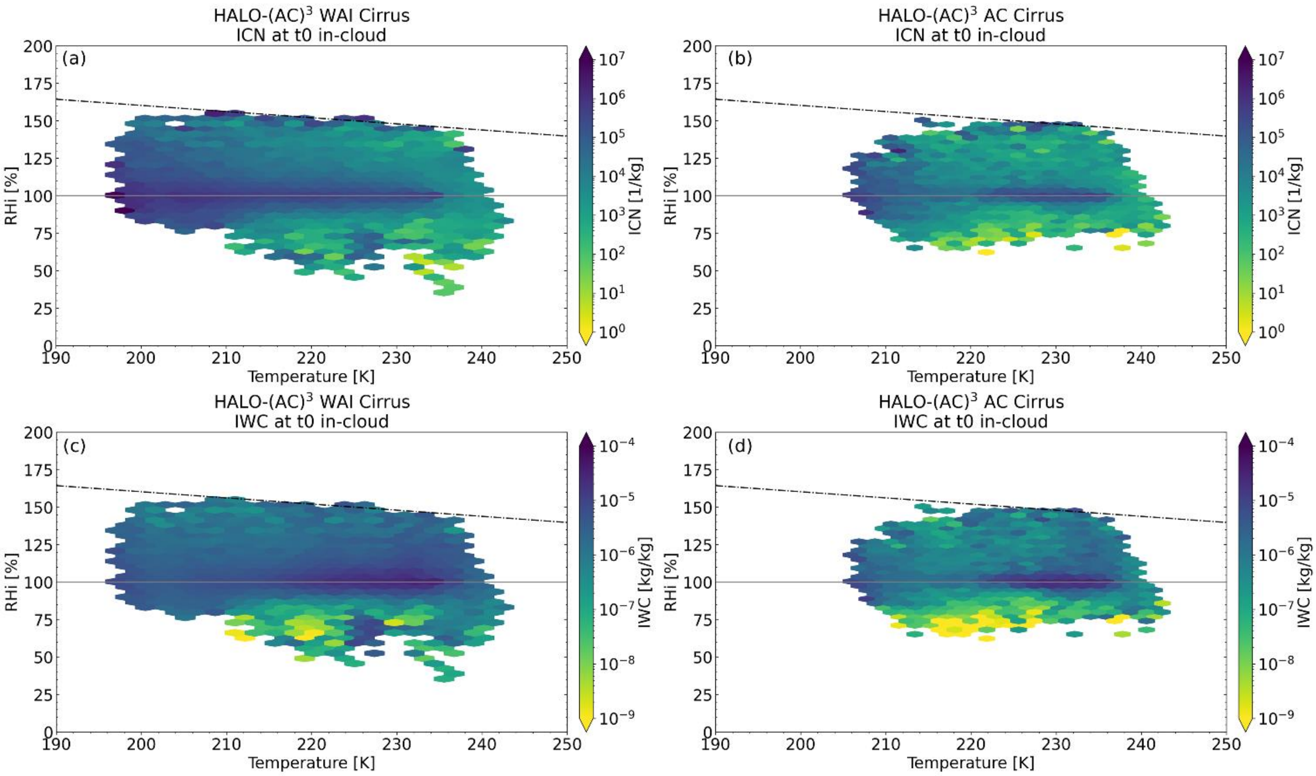

Figure 7: Comparison of ice microphysical properties from CLaMS-Ice, between Warm Air Intrusion (WAI Cirrus; Left) and Arctic Condition (AC Cirrus; Right) measured during the HALO-(AC)^3 campaign. The solid grey line depicts the threshold for ice saturation (RHi = 100 %). The black dash-dotted line represents the homogeneous nucleation (HOM) threshold based on Koop et al. (2000).

https://doi.org/10.5194/egusphere-2026-3788
Preprint. Discussion started: 13 August 2026

in both clouds, but more clearly for WAI cirrus, while AC cirrus have a region of high OD at cold temperatures and high ice supersaturation.

Moving on to the microphysical properties of AC and WAI cirrus at t0, for the Ice Water Content (IWC) we have three available data sources. The retrieval by VarCloud and calculations by CLaMS-Ice and LAGRANTO, all shown in Table 1. All sources point to a higher IWC in WAI cirrus, despite the exact values between them being different. CLaMS-Ice additionally classifies the nucleation pathway with which the reported IWC was created. For both cloud types HOM nucleation is the dominant ice nucleation process. HET nucleation is more common for AC than WAI cirrus. A possible explanation for this finding, is that in the model, WAI cirrus are more frequently found with pre-existing ice and are more likely to be classified as liquid origin, leading to less INP being available, since they are already in the ice crystals.

From VarCloud we also have the ice effective radius (R_{eff}). As shown in Table 1, AC cirrus have on average larger ice crystals, although WAI cirrus have the largest ice crystals. A detailed probability density plot is provided in Fig. 6 (b). Interestingly the distribution for the AC Cirrus has a double peak, which might be representative of the two ice nucleation processes, HOM and HET.

Finally, in Table 1, we also present the Ice Crystal Number concentration (ICN) as calculated by CLaMS-Ice. WAI cirrus are found to have a much greater ICN. Once again, the model provides the ice nucleation process, which took place, and similar to the IWC, HOM nucleation is the dominant process in both cloud types, while HET nucleation plays a more important role in AC compared to WAI cirrus. As already mentioned previously, in CLaMS-Ice WAI cirrus are frequently found with pre-existing ice, which could also have been HET and likely was.

In Fig. 7, we present a more detailed analysis of the ICN and IWC from CLaMS-Ice in the RHi-T space. Evidently and as expected, for both parameters and both cloud types, there are low values in subsaturation and the maxima are at around ice saturation (RHi = 100%). That being said, for the ICN both cloud types, have a double peak, one at warm and one at cold temperatures. For WAI cirrus the one at the colder end of the temperature range is dominant, whereas for AC cirrus the maximum ice crystal concentration at warmer temperatures is higher. The IWC appears to be rather similar between the two cloud types and also features a double maximum, although in this case both clouds have a stronger peak at warmer temperatures. Higher IWC values are detected in WAI cirrus in a broader RHi-T region.

3.3 Cloud classification based on formation and ice nucleation processes

In this final part of the statistical analysis we focus on the classification of the two cloud groups, based on their origin and initial ice nucleation process. Following the classification proposed by Krämer et al. (2016), cirrus can either form in situ at cold temperatures directly as ice clouds, or have a liquid predecessor, thus being classified as in-situ or liquid-origin. Both models, CLaMS-Ice and LAGRANTO, provide a cloud origin parameter.

In Fig. 8 we present our findings from the two models. According to the calculations by CLaMS-Ice, both AC and WAI cirrus are more frequently formed in-situ rather than have a liquid predecessor, but there are also strong differences. AC cirrus have 27.75 % of them being liquid-origin, while for WAI cirrus that percentage is lower, 16.89 %. The 'unknown origin/no-cloud'

https://doi.org/10.5194/egusphere-2026-3788
Preprint. Discussion started: 13 August 2026

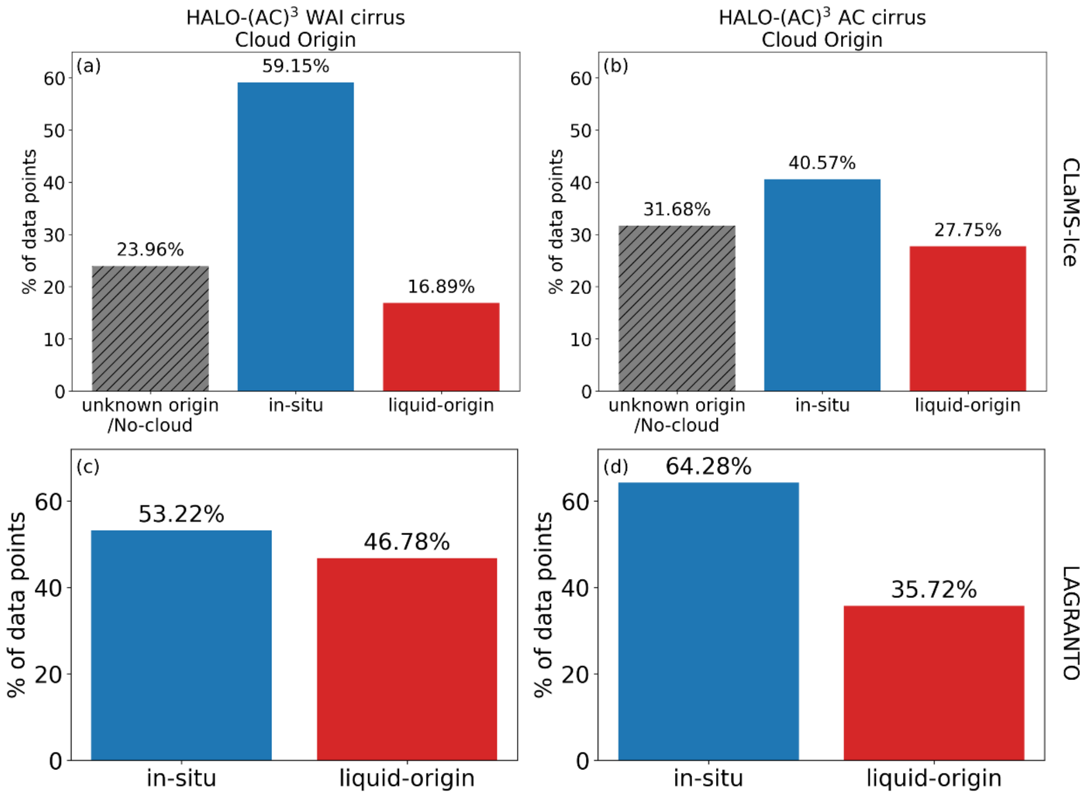

Figure 8: Cloud origin of Warm Air Intrusion (WAI Cirrus; Left) and Arctic Condition (AC Cirrus; Right) as calculated by CLaMS-Ice and LAGRANTO.

category, stems from the subsaturated, lower parts and most probably refers to evaporating cirrus with small IWC and ICN of unknown origin, or trajectories along which no cloud initiation threshold was passed.

The calculations from LAGRANTO are not in total agreement to those from CLaMS-Ice. Both models agree that AC as well as WAI cirrus are formed mostly in-situ, but LAGRANTO finds WAI cirrus clouds to have a larger liquid origin percentage compared to AC cirrus. The unknown origin category present only in CLaMS-Ice might affect the final result. The 2-moment microphysics scheme in CLaMS-Ice allows for the formation of an in-situ cirrus on a path where a liquid origin cirrus already existed and dissipated, which is also a common pathway in nature. In LAGRANTO this is not possible and once a liquid origin cloud has been detected it is registered as such until the end of the trajectory.

Using the HOM and HET nucleation pathways provided by CLaMS-Ice, we present the percentage at which each nucleation process takes place in the two cloud types. The results are shown in Fig. 9. We find, that HOM nucleation is the more frequent ice nucleation process for both cirrus types. HET nucleation takes place slightly more frequently in AC cirrus as compared to WAI cirrus. As was the case in the previous analysis, we also present our findings in the RHi-T space in Fig.

https://doi.org/10.5194/egusphere-2026-3788
Preprint. Discussion started: 13 August 2026

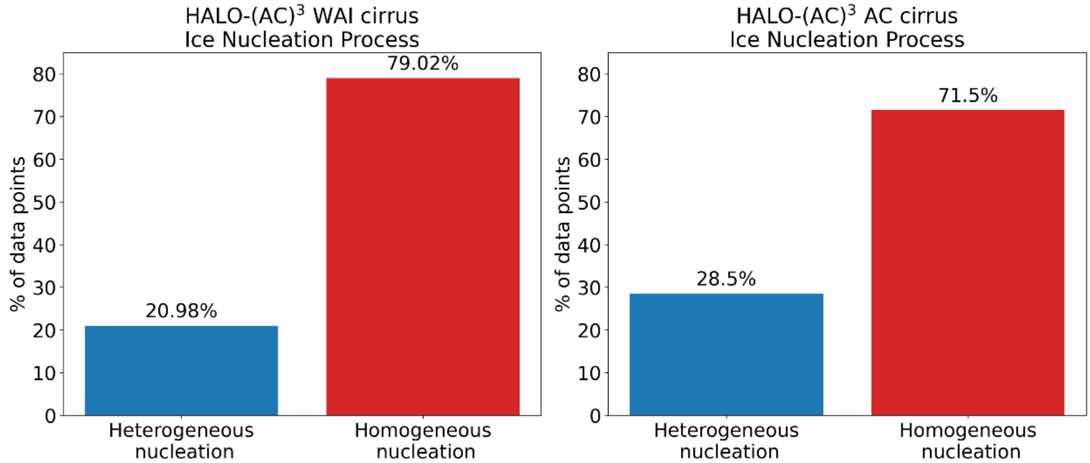

Figure 9: Comparison of ice nucleation processes between Warm Air Intrusion (WAI Cirrus; Left) and Arctic Condition (AC Cirrus; Right) as calculated by CLaMS-Ice data.

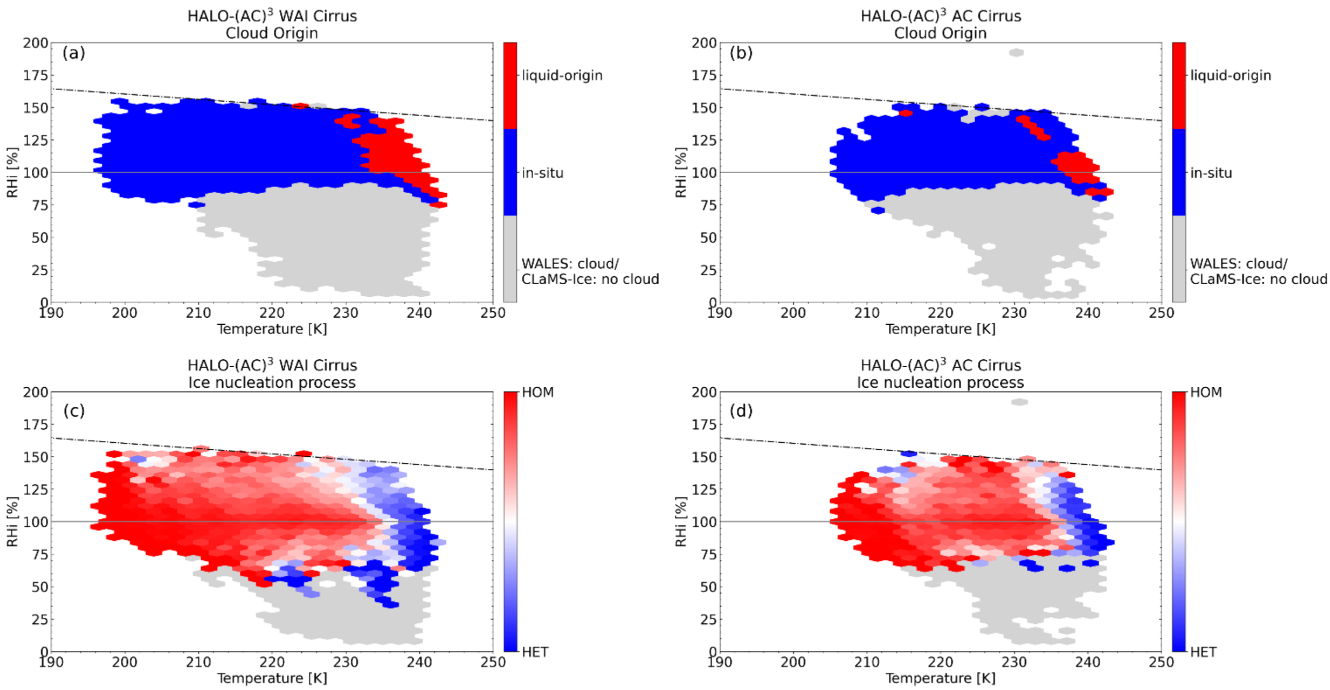

Figure 10: Comparison of cloud origin and ice nucleation prosses between Warm Air Intrusion (WAI Cirrus; Left) and Arctic Condition (AC Cirrus; Right) in the RHi-T space based on calculations from CLaMS-Ice. The solid grey line depicts the threshold for ice saturation (RHi = 100 %). The black dash-dotted line represents the homogeneous nucleation (HOM) threshold based on Koop et al. (2000).

10. Regarding the cloud origin, there is a definitive separation into three categories for both cloud types. The in-situ formed parts are dominant and found at most temperatures and RHi values, while the liquid-origin parts occupy only a small part of the warmest edge of the temperature range. Almost all data in subsaturated RHi, correspond to trajectories for which CLaMS-

https://doi.org/10.5194/egusphere-2026-3788
Preprint. Discussion started: 13 August 2026

Ice didn't detect cloud formation, whereas a cloud was detected in the WALES measurements. Regarding the ice nucleation processes, in both cloud types HOM nucleation is the dominant process and HET is found predominantly at warm temperatures in a wide range of super- and subsaturation. At these warmer temperatures the cirrus are more frequently of liquid-origin, where HET nucleation is prescribed in the model. The grey areas found at subsaturation come as a result of trajectories on which WALES did collect data characterised later as in-cloud, but CLaMS-Ice did not detect a cloud.

4 Discussion and conclusions

In the previous, we presented a detailed comparison of the optical, macro- and microphysical properties cirrus clouds formed during Warm Air Intrusions (WAI cirrus) and under Arctic Conditions (AC cirrus), based on remote sensing measurements and backwards trajectory analyses. In this section, our goal is to interpret these findings and explore the implications for cirrus cloud formation, evolution and impact in the Arctic.

The properties of ice clouds are subject to change with age and evolutionary stage, so comparison of clouds with different ages might introduce a bias. In our analysis, using both CLaMS-Ice and LAGRANTO we found that the median age of both WAI and AC cirrus is very similar to each other, despite the two models showing different ages, due to the difference in the calculation times. The cloud evolutionary stage might still differ between the clouds of the two groups, due to the different time scales in which the same or similar processes take place under varying ambient conditions (Krämer et al., 2009). The fact that the two cloud types have similar ages, removes one parameter and allows us to attribute their different properties to conditions and processes during their formation and evolution, rather than their different ages.

Further analysis of the cloud age in the RHi-T space (Fig. 3 (a) and (b), revealed that the older parts of the clouds in both cases, are found through a wide range of RHi at the colder part of the temperature range. That is an indication of old, long lived, ice crystals suspended in the clouds and transported to colder temperatures by the existing upwards motion. Younger parts were found mostly at warmer temperatures indicating freshly formed clouds in CLaMS-Ice, also due to upward transport. The youngest parts are found at very cold temperatures and very high supersaturations. This is a potential indication of HET and HOM nucleation respectively.

The nucleation process, HET or HOM can drastically change the properties of the final cirrus cloud. We consider HET nucleation to be the first one to take place, resulting in those ice crystals that formed early, to release latent heat, grow and sediment to lower parts of the clouds. HOM nucleation, requires high supersaturations at lower temperatures and follows HET nucleation if the required lifting is present. Thus, clouds that experience a stronger lifting would also have a higher contribution from HOM nucleation.

In order to verify this, the vertical motion was studied for the two cirrus types. We found that WAI cirrus experienced a stronger and faster vertical transport (Fig. 4 (a) and (b)). This finding was rather expected, when considering that the Arctic is mostly stable close to the tropopause under undisturbed conditions, while a WAI is characterized by upward motion. A stronger

https://doi.org/10.5194/egusphere-2026-3788
Preprint. Discussion started: 13 August 2026

upward transport of moisture leads airmasses to reach colder temperatures and higher supersaturations, allowing HOM nucleation, after all available INP have been activated via HET nucleation, a finding consistent also with Krämer et al. (2016). Having studied the conditions in the beginning and along the trajectories, we then focused on the optical, macro- and microphysical properties of the measured clouds at the time of detection. Starting with the macrophysical properties and more precisely the vertical extent, we found that WAI cirrus were on average geometrically thicker, with the difference stemming mostly from a higher cloud top. This is most probably connected with the stronger vertical motion present in WAI cirrus and can indicate on the one hand, that ice nucleation starts earlier and also on the other hand, that ice formation is ongoing for a longer time period, or at higher altitudes where HOM nucleation is dominant. This is also reflected in the RHi values measured in the two cirrus types (Fig. 5 (a)). WAI Cirrus are more frequently detected with RHi values that would support HOM nucleation.

Moving onto the optical properties, we looked into the optical depth of the two cirrus types (Fig. 2 (a) and (b)). We found, that AC cirrus are optically thinner, compared to WAI cirrus. In combination with the greater geometrical extent discussed above, this result is not surprising, but nevertheless it has important implications on the radiative properties of the two cloud types. Since WAI events have been found to be more frequent and long lasting, an increase on the frequency of detection of WAI cirrus might also lead to an alteration of the radiative effect they have in the Arctic.

The depolarization ratio, a parameter closely connecting the optical to the microphysical properties was the next one that we studied (Fig. 5 (b)). We found that WAI cirrus were on average detected with a higher depolarization ratio compared to AC cirrus. From this we can conclude, that WAI cirrus are made up of more complex shaped and larger ice crystals. This could be explained by an earlier onset of ice formation in WAI cirrus, most probably via HET nucleation. This, in combination with the sustained updrafts found in the WAI, and the release of latent heat during the HET nucleation, might lead to the ice crystals being suspended for a longer time period in moist, supersaturated air and thus growing bigger and more complex, and would also support the theory of HOM nucleation being the dominating process at the later stages of cloud formation at higher altitudes and lower temperatures.

For the next part of the analysis we focused on the microphysical properties of the clouds at the time of detection. First, we looked into the ice crystal number and effective radius (Figs. 6 and 7). These two parameters can provide a clearer insight into the nucleation process with which a cloud has formed. In general, HOM nucleation is expected to produce a larger number of smaller ice crystals, while HET nucleation results in a lower number of larger crystals (Comstock et al., 2008; Gasparini et al., 2018; Krämer et al., 2020). Keeping that in mind, we found that both cirrus types are detected with a relatively large range of ice crystal R_{eff} which could result from both HET and HOM nucleation. The distribution of R_{eff} for AC cirrus even presents a double peak, potentially the result of the two different nucleation processes (Fig. 6 (b)). Despite that, on average AC cirrus are found to have larger ice crystals, which might be an indication of HET nucleation being more dominant compared to WAI cirrus.

Moving on to the ICN, we found that WAI cirrus have on average a much higher ice crystal number concentration (Table 1). Since this parameter is provided by CLaMS-Ice, which has also a two-moment ice microphysics scheme, the additional information is provided, that most of the ice crystals for both clouds formed via HOM nucleation. HET nucleation is still present and is more frequently generating ice crystals in AC cirrus compared to WAI cirrus. The higher ICNs formed by HOM in the WAI are connected also to the higher updrafts, which generally cause many of the differences between WAI and AC cirrus (Krämer et al., 2020).

Summing up the findings from R_{eff} and ICN, WAI cirrus were found at the time of detection with slightly smaller ice crystals but in a larger number, whereas AC cirrus had slightly larger and fewer ice crystals. This is an indication of HOM nucleation being the more dominant process in WAI cirrus, while HET nucleation might have been more active in AC cirrus. This of course is the conclusion for the time of detection. Keeping in mind also all the other studied parameters, it is possible, that an initial formation of a large number of ice crystals via HET nucleation in WAI cirrus occured, while the stronger updrafts, possibly in combination with the released latent heat from that process, kept moving moist airmasses upwards to colder temperatures and higher supersaturations where HOM nucleation became the prevalent process, leading to the detected microphysical ice properties. Krämer et al. (2016, 2020) also detect a larger amount of small ice crystals resulting from HOM nucleation in clouds with faster updrafts, and few large ice crystals from HET nucleation in slower updrafts. The fact, that in WAI cirrus the largest amount of ice crystals is found at colder temperatures, near the cloud top, further supports this hypothesis. Simultaneously, this would mean, that the lower updrafts present for AC cirrus provided enough time for ice crystals to form on the fewer available INP and grow larger.

In the final part of our analysis we focused on the classification of the clouds based on their formation and nucleation process. From this analysis we confirmed HOM nucleation as the dominant process for both cloud types, with HET playing a more significant role in AC cirrus. For WAI cirrus the parts of the clouds that formed via HET nucleation are found only at warmer temperatures, a potential indication that they are older crystals that have already sedimented to the cloud base. In AC cirrus a small region at higher supersaturation and cold temperatures is found, where HET nucleation is responsible for ice formation. This could indicate that HET is an ongoing process parallel to HOM at the time of detection.

Regarding the formation process of the clouds, we found that both cirrus types form predominantly in-situ, i.e. directly as ice clouds, without a liquid predecessor. Regarding the liquid-origin parts, LAGRANTO and CLaMS-Ice come to different conclusions. LAGRANTO finds a higher percentage of liquid-origin in WAI cirrus, while CLaMS-Ice in AC.

5 Summary and outlook

In this study, we analysed and contrasted cirrus clouds that formed in the Arctic during Warm Air Intrusions (WAI cirrus) and under undisturbed Arctic Conditions (AC cirrus). We used lidar and radar observations from the HALO-$(AC)^3$ campaign as well as backward trajectory modelling. Our aim was to understand how the different ambient conditions and dynamical processes during cloud formation and evolution affect the properties of cirrus clouds in the Arctic.

We found that WAI cirrus experience stronger vertical transport along their trajectories lifting airmasses to the cold highly supersaturated regions where HOM nucleation is favoured. The analysis of the RHi confirmed, that WAI cirrus are more

https://doi.org/10.5194/egusphere-2026-3788
Preprint. Discussion started: 13 August 2026

frequently found at high supersaturations. WAI cirrus were also found to have a higher PLDR indicating more complex-shaped ice crystals.

Both cloud types form mostly in-situ and via the homogeneous ice nucleation process (HOM). HET nucleation is more common in AC cirrus compared to WAI cirrus, mainly due to the weaker, slower updrafts. The stronger updrafts present for WAI cirrus, combined with the release of latent heat from the initial HET nucleation, provide a sustained supply of moisture and transport airmasses to higher altitudes and colder temperatures supporting HOM nucleation.

At the time of detection, WAI cirrus were geometrically thicker and contained a larger number of smaller ice crystals, indicative of HOM nucleation. WAI cirrus are on average also optically thicker, which has implication on their radiative effect.

Our findings underscore the importance of dynamically driven cirrus formation processes and their sensitivity to aerosol loading and vertical transport and can be used to investigate biases in the representation of Arctic cirrus and the dynamical processes in the Arctic, potentially leading to improvements in weather predictions and climate projections in an ever-changing Arctic. Except for their intrinsic value, they also serve as a clear indication, that changes in the ambient conditions in the Arctic affect the properties of the cirrus clouds and form a basis from which more open questions can be investigated.

In future studies we aim to better quantify and connect the conditions during the formation and evolution of cirrus in the Arctic to their microphysical properties and especially to the radiative effects. Some questions to be investigated are for example how does the updraft speed affect the nucleation process and the ice crystal properties? What are the time scales of the processes that take place during cloud formation and evolution and how do they change under various ambient conditions? What is the cloud radiative forcing of cirrus with different formation pathways and microphysical properties? What are potential feedback mechanisms? An extension of the cirrus cloud database under various conditions and seasons is vital in this regard and can be done for example via remote sensing. Radiative transfer modelling is also an important tool towards answering many of these questions. In-situ observations of INP and microphysical properties of ice crystals, can also provide first a validation of the remote sensing measurements and some valuable insights on the properties and processes happening in the small scales (Murray et al., 2021).

Data availability

All data used in this study for the statistical analysis and graphs can be found in the following:

WALES lidar data: https://doi.org/10.1594/PANGAEA.967086 (Wirth and Groß, 2024)

VarCloud retrieval data: https://doi.org/10.5281/zenodo.20558488 (Ewald, 2026)

CLaMS-Ice and LAGRANTO data: https://doi.org/10.5281/zenodo.20431069 (Dekoutsidis et al., 2026)

Author contribution

The conceptualization of the study was undertaken by GD and SG. FE and MW curated the data, while MK, CR, and AS conducted the model simulations. GD performed the formal analysis, investigation, software implementation, and visualizations with contributions from all co-authors. The initial manuscript was drafted by GD, and all co-authors contributed to its review and editing.

Competing interests

At least one of the (co-)authors is a member of the editorial board of *Atmospheric Chemistry and Physics*.

Acknowledgements

This project has received funding from Horizon Europe programme under Grant Agreement No 101137680 via project CERTAINTY (Cloud-aERosol inTeractions & their impActs IN The earth sYstem). We thank the mission PI, coordinators, instruments operators, flight crews and technicians and everyone involved in the planning and execution of the HALO-(AC)3 campaign. We wholeheartedly thank Dr. Manuel Moser for his valuable input after reviewing this manuscript.

Financial support

The article processing charges for this open-access publication were covered by the German Aerospace Center (DLR).

References

Baumgartner, M., Rolf, C., Grooß, J.-U., Schneider, J., Schorr, T., Möhler, O., Spichtinger, P., and Krämer, M.: New investigations on homogeneous ice nucleation: the effects of water activity and water saturation formulations, Atmospheric Chemistry and Physics, 22, 65–91, https://doi.org/10.5194/acp-22-65-2022, 2022.

Cazenave, Q., Ceccaldi, M., Delanoë, J., Pelon, J., Groß, S., and Heymsfield, A.: Evolution of DARDAR-CLOUD ice cloud retrievals: new parameters and impacts on the retrieved microphysical properties, Atmospheric Measurement Techniques, 12, 2819–2835, https://doi.org/10.5194/amt-12-2819-2019, 2019.

Comstock, J. M., Lin, R.-F., Starr, D. O., and Yang, P.: Understanding ice supersaturation, particle growth, and number concentration in cirrus clouds, Journal of Geophysical Research: Atmospheres, 113, https://doi.org/10.1029/2008JD010332, 2008.

Costa, A.: Mixed-phase and ice cloud observations with NIXE-CAPS, Forschungszentrum Jülich GmbH Zentralbibliothek, Verlag, 2017.

https://doi.org/10.5194/egusphere-2026-3788
Preprint. Discussion started: 13 August 2026

Cziczo, D. J., Froyd, K. D., Hoose, C., Jensen, E. J., Diao, M., Zondlo, M. A., Smith, J. B., Twohy, C. H., and Murphy, D. M.: Clarifying the Dominant Sources and Mechanisms of Cirrus Cloud Formation, Science, 340, 1320–1324, https://doi.org/10.1126/science.1234145, 2013.

De La Torre Castro, E., Jurkat-Witschas, T., Afchine, A., Grewe, V., Hahn, V., Kirschler, S., Krämer, M., Lucke, J., Spelten, N., Wernli, H., Zöger, M., and Voigt, C.: Differences in microphysical properties of cirrus at high and mid-latitudes, Atmospheric Chemistry and Physics, 23, 13167–13189, https://doi.org/10.5194/acp-23-13167-2023, 2023.

Dekoutsidis, G., Groß, S., Wirth, M., Krämer, M., and Rolf, C.: Characteristics of supersaturation in midlatitude cirrus clouds and their adjacent cloud-free air, Atmospheric Chemistry and Physics, 23, 3103–3117, https://doi.org/10.5194/acp-23-3103-2023, 2023.

Dekoutsidis, G., Wirth, M., and Groß, S.: The effects of warm-air intrusions in the high Arctic on cirrus clouds, Atmospheric Chemistry and Physics, 24, 5971–5987, https://doi.org/10.5194/acp-24-5971-2024, 2024.

Dekoutsidis, G., Groß, S., Ewald, F., Krämer, M., Rolf, C., Schäfler, A., and Wirth, M.: Data for "Contrasting Arctic Cirrus Clouds: Properties and Processes from Observations and Simulations" by Dekoutsidis et al. 2026, 2026.

Delanoë, J. and Hogan, R. J.: A variational scheme for retrieving ice cloud properties from combined radar, lidar, and infrared radiometer, Journal of Geophysical Research: Atmospheres, 113, https://doi.org/10.1029/2007JD009000, 2008.

Delanoë, J. and Hogan, R. J.: Combined CloudSat-CALIPSO-MODIS retrievals of the properties of ice clouds, Journal of Geophysical Research: Atmospheres, 115, https://doi.org/10.1029/2009JD012346, 2010.

DeMott, P. J., Prenni, A. J., Liu, X., Kreidenweis, S. M., Petters, M. D., Twohy, C. H., Richardson, M. S., Eidhammer, T., and Rogers, D. C.: Predicting global atmospheric ice nuclei distributions and their impacts on climate, Proceedings of the National Academy of Sciences, 107, 11217–11222, https://doi.org/10.1073/pnas.0910818107, 2010.

Ehrlich, A., Crewell, S., Herber, A., Klingebiel, M., Lüpkes, C., Mech, M., Becker, S., Borrmann, S., Bozem, H., Buschmann, M., Clemen, H.-C., De La Torre Castro, E., Dorff, H., Dupuy, R., Eppers, O., Ewald, F., George, G., Giez, A., Grawe, S., Gourbeyre, C., Hartmann, J., Jäkel, E., Joppe, P., Jourdan, O., Jurányi, Z., Kirbus, B., Lucke, J., Luebke, A. E., Maahn, M., Maherndl, N., Mallaun, C., Mayer, J., Mertes, S., Mioche, G., Moser, M., Müller, H., Pörtge, V., Risse, N., Roberts, G., Rosenburg, S., Röttenbacher, J., Schäfer, M., Schaefer, J., Schäfler, A., Schirmacher, I., Schneider, J., Schnitt, S., Stratmann, F., Tatzelt, C., Voigt, C., Walbröl, A., Weber, A., Wetzel, B., Wirth, M., and Wendisch, M.: A comprehensive in situ and remote sensing data set collected during the HALO–($\mathcal{A}$ $\mathcal{C}$)^3 aircraft campaign, Earth System Science Data, 17, 1295–1328, https://doi.org/10.5194/essd-17-1295-2025, 2025.

Ewald, F.: Varcloud ice cloud properties (Level 2B) derived from HALO data obtained during the (AC)3 campaign, https://doi.org/10.5281/ZENODO.20558488, 2026.

Ewald, F., Groß, S., Hagen, M., Hirsch, L., Delanoë, J., and Bauer-Pfundstein, M.: Calibration of a 35 GHz airborne cloud radar: lessons learned and intercomparisons with 94 GHz cloud radars, Atmospheric Measurement Techniques, 12, 1815–1839, https://doi.org/10.5194/amt-12-1815-2019, 2019.

Ewald, F., Groß, S., Wirth, M., Delanoë, J., Fox, S., and Mayer, B.: Why we need radar, lidar, and solar radiance observations to constrain ice cloud microphysics, Atmospheric Measurement Techniques, 14, 5029–5047, https://doi.org/10.5194/amt-14-5029-2021, 2021.

https://doi.org/10.5194/egusphere-2026-3788
Preprint. Discussion started: 13 August 2026

Gasparini, B., Meyer, A., Neubauer, D., Münch, S., and Lohmann, U.: Cirrus Cloud Properties as Seen by the CALIPSO Satellite and ECHAM-HAM Global Climate Model, Journal of Climate, 31, 1983–2003, https://doi.org/10.1175/JCLI-D-16-0608.1, 2018.

Graham, R. M., Cohen, L., Petty, A. A., Boisvert, L. N., Rinke, A., Hudson, S. R., Nicolaus, M., and Granskog, M. A.: Increasing frequency and duration of Arctic winter warming events, Geophysical Research Letters, 44, 6974–6983, https://doi.org/10.1002/2017GL073395, 2017.

Groß, S., Wirth, M., Schäfler, A., Fix, A., Kaufmann, S., and Voigt, C.: Potential of airborne lidar measurements for cirrus cloud studies, Atmospheric Measurement Techniques, 7, 2745–2755, https://doi.org/10.5194/amt-7-2745-2014, 2014.

Hoose, C. and Möhler, O.: Heterogeneous ice nucleation on atmospheric aerosols: a review of results from laboratory experiments, Atmospheric Chemistry and Physics, 12, 9817–9854, https://doi.org/10.5194/acp-12-9817-2012, 2012.

Intrieri, J. M., Fairall, C. W., Shupe, M. D., Persson, P. O. G., Andreas, E. L., Guest, P. S., and Moritz, R. E.: An annual cycle of Arctic surface cloud forcing at SHEBA, Journal of Geophysical Research: Oceans, 107, SHE 13-1-SHE 13-14, https://doi.org/10.1029/2000JC000439, 2002.

Johansson, E., Devasthale, A., Tjernström, M., Ekman, A. M. L., and L'Ecuyer, T.: Response of the lower troposphere to moisture intrusions into the Arctic, Geophysical Research Letters, 44, 2527–2536, https://doi.org/10.1002/2017GL072687, 2017.

Kärcher, B. and Lohmann, U.: A parameterization of cirrus cloud formation: Homogeneous freezing of supercooled aerosols, Journal of Geophysical Research: Atmospheres, 107, AAC 4-1-AAC 4-10, https://doi.org/10.1029/2001JD000470, 2002.

Kärcher, B. and Lohmann, U.: A parameterization of cirrus cloud formation: Heterogeneous freezing, Journal of Geophysical Research: Atmospheres, 108, https://doi.org/10.1029/2002JD003220, 2003.

Koop, T., Luo, B., Tsias, A., and Peter, T.: Water activity as the determinant for homogeneous ice nucleation in aqueous solutions, Nature, 406, 611–614, https://doi.org/10.1038/35020537, 2000.

Krämer, M., Schiller, C., Afchine, A., Bauer, R., Gensch, I., Mangold, A., Schlicht, S., Spelten, N., Sitnikov, N., Borrmann, S., de Reus, M., and Spichtinger, P.: Ice supersaturations and cirrus cloud crystal numbers, Atmospheric Chemistry and Physics, 9, 3505–3522, https://doi.org/10.5194/acp-9-3505-2009, 2009.

Krämer, M., Rolf, C., Luebke, A., Afchine, A., Spelten, N., Costa, A., Meyer, J., Zöger, M., Smith, J., Herman, R. L., Buchholz, B., Ebert, V., Baumgardner, D., Borrmann, S., Klingebiel, M., and Avallone, L.: A microphysics guide to cirrus clouds – Part 1: Cirrus types, Atmospheric Chemistry and Physics, 16, 3463–3483, https://doi.org/10.5194/acp-16-3463-2016, 2016.

Krämer, M., Rolf, C., Spelten, N., Afchine, A., Fahey, D., Jensen, E., Khaykin, S., Kuhn, T., Lawson, P., Lykov, A., Pan, L. L., Riese, M., Rollins, A., Stroh, F., Thornberry, T., Wolf, V., Woods, S., Spichtinger, P., Quaas, J., and Sourdeval, O.: A microphysics guide to cirrus – Part 2: Climatologies of clouds and humidity from observations, Atmospheric Chemistry and Physics, 20, 12569–12608, https://doi.org/10.5194/acp-20-12569-2020, 2020.

Krautstrunk, M. and Giez, A.: The Transition From FALCON to HALO Era Airborne Atmospheric Research, in: Atmospheric Physics: Background – Methods – Trends, edited by: Schumann, U., Springer, Berlin, Heidelberg, 609–624, https://doi.org/10.1007/978-3-642-30183-4_37, 2012.

https://doi.org/10.5194/egusphere-2026-3788
Preprint. Discussion started: 13 August 2026

Luebke, A. E., Avallone, L. M., Schiller, C., Meyer, J., Rolf, C., and Krämer, M.: Ice water content of Arctic, midlatitude, and tropical cirrus – Part 2: Extension of the database and new statistical analysis, Atmospheric Chemistry and Physics, 13, 6447–6459, https://doi.org/10.5194/acp-13-6447-2013, 2013.

Luebke, A. E., Afchine, A., Costa, A., Grooß, J.-U., Meyer, J., Rolf, C., Spelten, N., Avallone, L. M., Baumgardner, D., and Krämer, M.: The origin of midlatitude ice clouds and the resulting influence on their microphysical properties, Atmos. Chem. Phys., 16, 5793–5809, https://doi.org/10.5194/acp-16-5793-2016, 2016.

Lynch, D. K.: Cirrus, Oxford University Press, 499 pp., 2002.

Marsing, A., Meerkötter, R., Heller, R., Kaufmann, S., Jurkat-Witschas, T., Krämer, M., Rolf, C., and Voigt, C.: Investigating the radiative effect of Arctic cirrus measured in situ during the winter 2015–2016, Atmospheric Chemistry and Physics, 23, 587–609, https://doi.org/10.5194/acp-23-587-2023, 2023.

McKenna, D. S., Konopka, P., Grooß, J.-U., Günther, G., Müller, R., Spang, R., Offermann, D., and Orsolini, Y.: A new Chemical Lagrangian Model of the Stratosphere (CLaMS) 1. Formulation of advection and mixing, Journal of Geophysical Research: Atmospheres, 107, ACH 15-1-ACH 15-15, https://doi.org/10.1029/2000JD000114, 2002.

Mech, M., Orlandi, E., Crewell, S., Ament, F., Hirsch, L., Hagen, M., Peters, G., and Stevens, B.: HAMP – the microwave package on the High Altitude and LOng range research aircraft (HALO), Atmospheric Measurement Techniques, 7, 4539–4553, https://doi.org/10.5194/amt-7-4539-2014, 2014.

Mitchell, D. L., Garnier, A., Pelon, J., and Erfani, E.: CALIPSO (IIR–CALIOP) retrievals of cirrus cloud ice-particle concentrations, Atmospheric Chemistry and Physics, 18, 17325–17354, https://doi.org/10.5194/acp-18-17325-2018, 2018.

Mitchell, D. L., Mejia, J., Garnier, A., Tomii, Y., Krämer, M., and Hosseinpour, F.: An Estimate of Global, Regional and Seasonal Cirrus Cloud Radiative Effects Contributed by Homogeneous Ice Nucleation, Atmospheric Chemistry and Physics Discussions, 1–48, https://doi.org/10.5194/acp-2020-846, 2020.

Murray, B. J., Carslaw, K. S., and Field, P. R.: Opinion: Cloud-phase climate feedback and the importance of ice-nucleating particles, Atmospheric Chemistry and Physics, 21, 665–679, https://doi.org/10.5194/acp-21-665-2021, 2021.

Pithan, F., Svensson, G., Caballero, R., Chechin, D., Cronin, T. W., Ekman, A. M. L., Neggers, R., Shupe, M. D., Solomon, A., Tjernström, M., and Wendisch, M.: Role of air-mass transformations in exchange between the Arctic and mid-latitudes, Nature Geosci, 11, 805–812, https://doi.org/10.1038/s41561-018-0234-1, 2018.

Podglajen, A., Hertzog, A., Plougonven, R., and Legras, B.: Lagrangian temperature and vertical velocity fluctuations due to gravity waves in the lower stratosphere, Geophysical Research Letters, 43, 3543–3553, https://doi.org/10.1002/2016GL068148, 2016.

Richter-Menge, J., Jeffries, M. O., and Osborne, E.: 5. THE ARCTIC., Bulletin of the American Meteorological Society, 99, S143–S143, 2018.

Schäfler, A., Sprenger, M., Wernli, H., Fix, A., and Wirth, M.: Case study on the influence of synoptic-scale processes on the paired H_2 O–O_3 distribution in the UTLS across a North Atlantic jet stream, Atmos. Chem. Phys., 23, 999–1018, https://doi.org/10.5194/acp-23-999-2023, 2023.

Serreze, M. C. and Francis, J. A.: The Arctic Amplification Debate, Climatic Change, 76, 241–264, https://doi.org/10.1007/s10584-005-9017-y, 2006.

https://doi.org/10.5194/egusphere-2026-3788
Preprint. Discussion started: 13 August 2026

Shupe, M. D. and Intrieri, J. M.: Cloud Radiative Forcing of the Arctic Surface: The Influence of Cloud Properties, Surface Albedo, and Solar Zenith Angle, Journal of Climate, 17, 616–628, https://doi.org/10.1175/1520-0442(2004)017<0616:CRFOTA>2.0.CO;2, 2004.

Spichtinger, P. and Gierens, K. M.: Modelling of cirrus clouds – Part 1a: Model description and validation, Atmospheric Chemistry and Physics, 9, 685–706, https://doi.org/10.5194/acp-9-685-2009, 2009.

Sprenger, M. and Wernli, H.: The LAGRANTO Lagrangian analysis tool – version 2.0, Geosci. Model Dev., 8, 2569–2586, https://doi.org/10.5194/gmd-8-2569-2015, 2015.

Stendel, M., Francis, J., White, R., Williams, P. D., and Woollings, T.: Chapter 15 - The jet stream and climate change, in: Climate Change (Third Edition), edited by: Letcher, T. M., Elsevier, 327–357, https://doi.org/10.1016/B978-0-12-821575-3.00015-3, 2021.

Stephens, G. L., Vane, D. G., Tanelli, S., Im, E., Durden, S., Rokey, M., Reinke, D., Partain, P., Mace, G. G., Austin, R., L'Ecuyer, T., Haynes, J., Lebsock, M., Suzuki, K., Waliser, D., Wu, D., Kay, J., Gettelman, A., Wang, Z., and Marchand, R.: CloudSat mission: Performance and early science after the first year of operation, Journal of Geophysical Research: Atmospheres, 113, https://doi.org/10.1029/2008JD009982, 2008.

Stevens, B., Ament, F., Bony, S., Crewell, S., Ewald, F., Gross, S., Hansen, A., Hirsch, L., Jacob, M., Kölling, T., Konow, H., Mayer, B., Wendisch, M., Wirth, M., Wolf, K., Bakan, S., Bauer-Pfundstein, M., Brueck, M., Delanoë, J., Ehrlich, A., Farrell, D., Forde, M., Gödde, F., Grob, H., Hagen, M., Jäkel, E., Jansen, F., Klepp, C., Klingebiel, M., Mech, M., Peters, G., Rapp, M., Wing, A. A., and Zinner, T.: A High-Altitude Long-Range Aircraft Configured as a Cloud Observatory: The NARVAL Expeditions, Bulletin of the American Meteorological Society, 100, 1061–1077, https://doi.org/10.1175/BAMS-D-18-0198.1, 2019.

Urbanek, B., Groß, S., Schäfler, A., and Wirth, M.: Determining stages of cirrus evolution: a cloud classification scheme, Atmospheric Measurement Techniques, 10, 1653–1664, https://doi.org/10.5194/amt-10-1653-2017, 2017.

Urbanek, B., Groß, S., Wirth, M., Rolf, C., Krämer, M., and Voigt, C.: High Depolarization Ratios of Naturally Occurring Cirrus Clouds Near Air Traffic Regions Over Europe, Geophysical Research Letters, 45, 13,166-13,172, https://doi.org/10.1029/2018GL079345, 2018.

Wendisch, M., Brückner, M., Crewell, S., Ehrlich, A., Notholt, J., Lüpkes, C., Macke, A., Burrows, J. P., Rinke, A., Quaas, J., Maturilli, M., Schemann, V., Shupe, M. D., Akansu, E. F., Barrientos-Velasco, C., Bärfuss, K., Blechschmidt, A.-M., Block, K., Bougoudis, I., Bozem, H., Böckmann, C., Bracher, A., Bresson, H., Bretschneider, L., Buschmann, M., Chechin, D. G., Chylik, J., Dahlke, S., Deneke, H., Dethloff, K., Donth, T., Dorn, W., Dupuy, R., Ebell, K., Egerer, U., Engelmann, R., Eppers, O., Gerdes, R., Gierens, R., Gorodetskaya, I. V., Gottschalk, M., Griesche, H., Gryanik, V. M., Handorf, D., Harm-Altstädter, B., Hartmann, J., Hartmann, M., Heinold, B., Herber, A., Herrmann, H., Heygster, G., Höschel, I., Hofmann, Z., Hölemann, J., Hünerbein, A., Jafariserajehlou, S., Jäkel, E., Jacobi, C., Janout, M., Jansen, F., Jourdan, O., Jurányi, Z., Kalesse-Los, H., Kanzow, T., Käthner, R., Kliesch, L. L., Klingebiel, M., Knudsen, E. M., Kovács, T., Körtke, W., Krampe, D., Kretzschmar, J., Kreyling, D., Kulla, B., Kunkel, D., Lampert, A., Lauer, M., Lelli, L., Lerber, A. von, Linke, O., Löhnert, U., Lonardi, M., Losa, S. N., Losch, M., Maahn, M., Mech, M., Mei, L., Mertes, S., Metzner, E., Mewes, D., Michaelis, J., Mioche, G., Moser, M., Nakoudi, K., Neggers, R., Neuber, R., Nomokonova, T., Oelker, J., Papakonstantinou-Presvelou, I., et al.: Atmospheric and Surface Processes, and Feedback Mechanisms Determining Arctic Amplification: A Review of First Results and Prospects of the (AC)3 Project, Bulletin of the American Meteorological Society, 104, E208–E242, https://doi.org/10.1175/BAMS-D-21-0218.1, 2023.

Wendisch, M., Crewell, S., Ehrlich, A., Herber, A., Kirbus, B., Lüpkes, C., Mech, M., Abel, S. J., Akansu, E. F., Ament, F., Aubry, C., Becker, S., Borrmann, S., Bozem, H., Brückner, M., Clemen, H.-C., Dahlke, S., Dekoutsidis, G., Delanoë, J., De

La Torre Castro, E., Dorff, H., Dupuy, R., Eppers, O., Ewald, F., George, G., Gorodetskaya, I. V., Grawe, S., Groß, S., Hartmann, J., Henning, S., Hirsch, L., Jäkel, E., Joppe, P., Jourdan, O., Jurányi, Z., Karalis, M., Kellermann, M., Klingebiel, M., Lonardi, M., Lucke, J., Luebke, A. E., Maahn, M., Maherndl, N., Maturilli, M., Mayer, B., Mayer, J., Mertes, S., Michaelis, J., Michalkov, M., Mioche, G., Moser, M., Müller, H., Neggers, R., Ori, D., Paul, D., Paulus, F. M., Pilz, C., Pithan, F., Pöhlker, M., Pörtge, V., Ringel, M., Risse, N., Roberts, G. C., Rosenburg, S., Röttenbacher, J., Rückert, J., Schäfer, M., Schaefer, J., Schemann, V., Schirmacher, I., Schmidt, J., Schmidt, S., Schneider, J., Schnitt, S., Schwarz, A., Siebert, H., Sodemann, H., Sperzel, T., Spreen, G., Stevens, B., Stratmann, F., Svensson, G., Tatzelt, C., Tuch, T., Vihma, T., Voigt, C., Volkmer, L., Walbröl, A., Weber, A., Wehner, B., Wetzel, B., Wirth, M., and Zinner, T.: Overview: quasi-Lagrangian observations of Arctic air mass transformations – introduction and initial results of the HALO–$(\mathcal{AC})^3$ aircraft campaign, Atmospheric Chemistry and Physics, 24, 8865–8892, https://doi.org/10.5194/acp-24-8865-2024, 2024.

Wendisch, M., Kirbus, B., Ori, D., Shupe, M. D., Crewell, S., Sodemann, H., and Schemann, V.: Observed and modeled Arctic airmass transformations during warm air intrusions and cold air outbreaks, Atmospheric Chemistry and Physics, 25, 15047–15076, 2025.

Wernli, H. and Davies, H. C.: A Lagrangian-based analysis of extratropical cyclones. I: The method and some applications, Quarterly Journal of the Royal Meteorological Society, 123, 467–489, https://doi.org/10.1002/qj.49712353811, 1997.

Wernli, H., Boettcher, M., Joos, H., Miltenberger, A. K., and Spichtinger, P.: A trajectory-based classification of ERA-Interim ice clouds in the region of the North Atlantic storm track, Geophysical Research Letters, 43, 6657–6664, https://doi.org/10.1002/2016GL068922, 2016.

Winker, D. M., Pelon, J., Coakley, J. A., Ackerman, S. A., Charlson, R. J., Colarco, P. R., Flamant, P., Fu, Q., Hoff, R. M., Kittaka, C., Kubar, T. L., Treut, H. L., Mccormick, M. P., Mégie, G., Poole, L., Powell, K., Trepte, C., Vaughan, M. A., and Wielicki, B. A.: The CALIPSO Mission: A Global 3D View of Aerosols and Clouds, Bulletin of the American Meteorological Society, 91, 1211–1230, https://doi.org/10.1175/2010BAMS3009.1, 2010.

Wirth, M. and Groß, S.: Aircraft measurements of backscatter ratio, particle depolarization and water vapour molecular density profiles over Arctic sea ice and ocean during the HALO-$(AC)^3$ campaign in spring 2022, https://doi.org/10.1594/PANGAEA.967086, 2024.

Wirth, M., Fix, A., Mahnke, P., Schwarzer, H., Schrandt, F., and Ehret, G.: The airborne multi-wavelength water vapor differential absorption lidar WALES: system design and performance, Appl. Phys. B, 96, 201–213, https://doi.org/10.1007/s00340-009-3365-7, 2009.

Woods, C. and Caballero, R.: The Role of Moist Intrusions in Winter Arctic Warming and Sea Ice Decline, Journal of Climate, 29, 4473–4485, https://doi.org/10.1175/JCLI-D-15-0773.1, 2016.